Solvent Effects on the Self-Association of Formic Acid in Carbon Dioxide and Ethane

YoonKook Park,[†] Ram B. Gupta,[‡] Christine W. Curtis,[‡] and Christopher B. Roberts*[,‡]

Chemical Engineering Departments, Tuskegee University, Tuskegee, Alabama 36088, and Auburn University, Auburn, Alabama 36849

Received: February 19, 2002; In Final Form: June 17, 2002

The association of formic acid in both carbon dioxide and ethane at 298−318 K and 48−100 bar has been studied using Fourier transform infrared (FTIR) spectroscopy. The equilibrium constant, *K*, between dimer and monomer of the formic acid was obtained by examination of the carbonyl stretching band for formic acid. The concentrations of formic acid studied ranged from 1.0 to 8.4 mmol/L. In general, the results show that an increase in density causes an increase in the concentration of the formic acid monomer, which results in a decrease in *K*. The dimerization constant is significantly higher in ethane than in carbon dioxide. This result is a consequence of an enhanced interaction between formic acid (solute) and carbon dioxide (solvent) compared to the interaction between formic acid (solute) and ethane (solvent). Furthermore, the modified lattice-fluid hydrogen-bonding model (MLFHB) has been used to interpret the effects of density on the *K*. The influence of the carbon dioxide and ethane solvents on the equilibrium behavior of the formic acid is discussed in terms of the role of the solvent density and specific solute−solvent interactions.

1. Introduction

A carboxylic acid is an interesting species because it contains both a carbonyl group and a hydroxyl group; the interaction of these two groups lead to an intramolecular hydrogen bond that is unique to carboxylic acids. Among them, formic acid is industrially important by itself as it plays a well-known prominent role in human metabolism.[1] Since saturated carboxylic acids containing carbonyl groups represent good examples of intramolecular hydrogen bonds, a few researchers have studied the self-association equilibria of carboxylic acids.[2−6]

Fourier transform infrared (FTIR) spectroscopy has been shown to be useful for the characterization of molecular interactions. Fulton et al.[7] used FTIR spectroscopy to measure the degree of self-association of deuterated methanol solute molecules in supercritical CO_2, supercritical ethane, and liquid heptane. Their results show that CO_2 solvent shifts the self-association equilibrium of methanol-*d* toward the monomer form of the alcohol, whereas the use of supercritical ethane and liquid heptane solvents favors the formation of methanol-*d* clusters. They attributed this behavior to a chemical complex between methanol-*d* and CO_2.

Recently, Yamamoto et al.[6] determined the equilibrium constants of the dimerization for carboxylic acid (acetic acid and plamitic acid) and the amount of hydrogen-bonding species between carboxylic acid and ethanol in supercritical CO_2 by using the carbonyl stretching band for carboxylic acid. In the carboxylic acid and supercritical CO_2 system, they considered the solvent effect on the basis of the equilibrium constants of the dimerization between carboxylic acid dimer and monomer. The dimerization constants in the organic liquid solvent (benzene, toluene, chloroform, etc.) are larger than those in supercritical CO_2. This fact indicates that the monomeric form carboxylic acid is more stable in supercritical CO_2 than in the organic liquid solvents, because the interaction between CO_2 and carboxylic acid is stronger than that between nonpolar or weakly polar organic solvents and carboxylic acid.[6]

In this study, FTIR spectroscopy is used to determine the equilibrium constants of dimerization between formic acid dimer and monomer in sub- and supercritical CO_2. The effect of CO_2 density on dimerization of formic acid was investigated by varying temperature and pressure. Additionally, changing the solvent to ethane allows the examination of the effect of the solvent type on formic acid dimerization. Furthermore, the equilibrium constants spectroscopically obtained are used directly in the modified lattice-fluid hydrogen-bonding (MLFHB) model.

2. Experimental Section

2.1. Materials. Formic acid of 98−100% (cat. no. 27001) was purchased from Sigma and used without further purification. SFC grade carbon dioxide from BOC Gases has a reported purity of 99.999% and was used as received. Research grade ethane was purchased from BOC gases and was purified with a gas drier (Alltech, part no. 8113) before use.

2.2. Apparatus and Procedure. The experimental apparatus, as shown in Figure 1, consisted of an Isco 260D syringe pump equipped with a water jacket to control the solvent temperature, a metering pump (Eldex Laboratories Inc. model no. B-100-S), a six port injection valve (Valco), a temperature controller (Omega 6071A controller with an RTD), a digital pressure indicator (Heise model 901A), and a custom high-pressure FTIR cell. The system was connected and compartmentalized using 1/16″ stainless steel tubing and high-pressure valves purchased from High-Pressure Equipment Co. (Erie, PA).

The custom FTIR cell was constructed from 316 stainless steel and was equipped with ZnSe windows. The volume and optical path length of the high-pressure cell were 1.4 cm^3 and 0.28 cm, respectively. A schematic of the cross-sectional view of the high-pressure cell is shown in Figure 2. ZnSe windows

* To whom correspondence should be addressed. Phone: 334-844-2036. Fax: 334-844-2063. E-mail: croberts@eng.auburn.edu.
[†] Tuskegee University.
[‡] Auburn University.

10.1021/jp020447p CCC: $22.00
Published on Web 08/24/2002

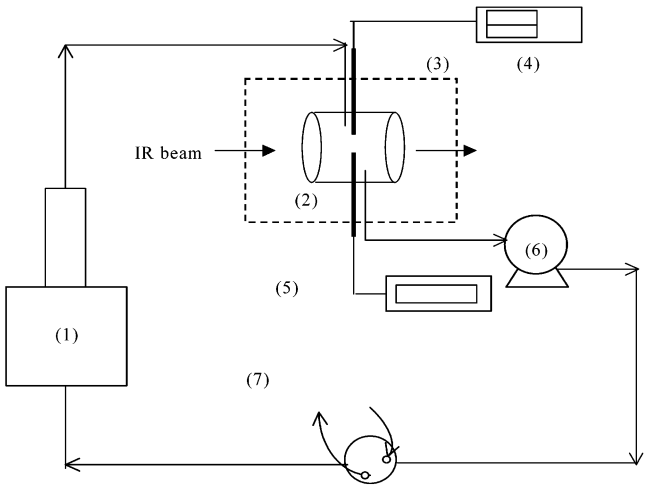

Figure 1. Experimental setup for high-pressure FTIR measurements: (1) syringe pump; (2) high-pressure cell; (3) FTIR sample chamber; (4) temperature controller; (5) pressure transducer; (6) metering pump; (7) injection valve.

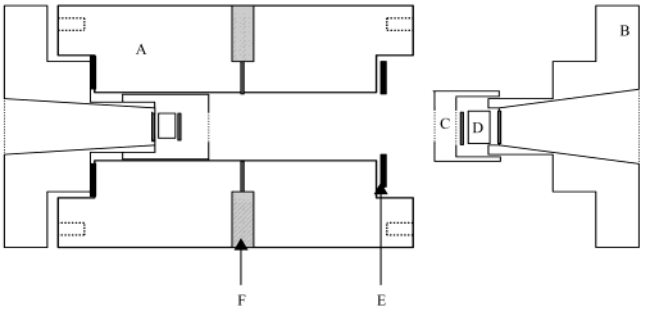

Figure 2. Schematic diagram of a high-pressure cell: A, housing; B, window holder; C, cap; D, ZnSe window; E, lead sheet; F, inlet, outlet temperature, and pressure port.

were obtained from Harrick Scientific, and the window dimensions employed were 6 mm diameter and 13 mm thickness. An indium foil (cat. no. 26,405-9) was obtained from Aldrich and used to form the seal between the window holder and cap. Lead seal rings were fashioned from a 1/24″ lead sheet (cat. no. 9032K119, 12″ × 24″) which was purchased from McMaster-Carr and used to form the seal between window holder and the cell housing.

Initially, the syringe pump was purged with CO_2 to remove moisture from the system and then charged with a known amount of CO_2. The remainder of the system was purged with dry nitrogen and connected to the syringe pump. The syringe pump was set to the desired pressure, and the desired temperature was maintained with a water jacket. The system was then pressurized using the syringe pump, and a metering pump was used to continuously recirculate the solution through the system including the FTIR cell and the injection valve. To maintain constant temperature in the FTIR cell, the high-pressure cell was wrapped with flexible heaters purchased from Omega (cat. no. KH-106/5-P). A temperature controller equipped with an RTD temperature probe maintained the solution temperature in the high-pressure IR cell to within 0.1 °C. Before the formic acid was introduced into the system, a baseline FTIR spectrum was collected. The six-port injector allowed the addition of fixed amounts of the formic acid into the system without the risk of loss of solution or contamination by atmospheric moisture. In the case of CO_2, 10 μL injections of formic acid were introduced stepwise, and 2 μL stepwise injections of formic acid were used in the case of ethane solvent. After each injection of formic acid was introduced (up to 5 total injections), the system was allowed to equilibrate at the desired temperature and pressure. Once equilibrium was achieved, typically less than 30 min, FTIR spectra were collected for analysis. All spectra were recorded with a Perkin-Elmer Spectra 2000 FTIR spectrometer and consisted of 100 averaged scans at 8 cm^{-1} resolution. The FTIR spectrometer was purged with dry nitrogen (BOC gases grade 5.0) before collecting all infrared spectra to eliminate atmospheric interference. The FTIR spectra were used for analysis as described below. After the FTIR spectra were collected at a given formic acid concentration, the above injection procedure was subsequently repeated up to a total of 5 injections at each temperature and pressure studied. In other words, the maximum amount of formic acid injected in CO_2 was 50 μL and was 10 μL in ethane.

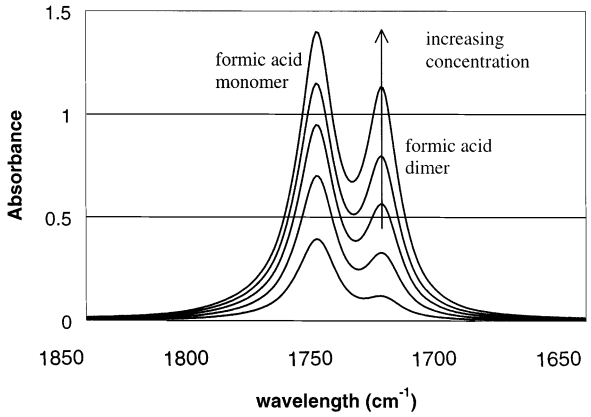

Figure 3. FTIR spectra of the C═O stretching band for formic acid in carbon dioxide at 303 K and 88 bar.

For these experiments, temperatures of 25−45 °C and pressures of 48−100 bar were examined because these temperatures and pressures covered an appropriate range for the sub- and supercritical CO_2 (T_c = 31 °C, P_c = 74 bar, ρ_c =0.49 g/cm^3) and ethane (T_c = 32 °C, P_c = 49 bar, ρ_c = 0.20 g/cm^3). The concentrations of formic acid studied (on the basis of the injection procedure above) ranged from 1.0 to 8.4 mmol/L. These formic acid concentrations were chosen to keep the total absorbance of the carbonyl bands less than 2. In addition, these concentrations of formic acid are sufficiently low such that the mixture densities were estimated to be those of the pure solvents (CO_2 or ethane) at the given temperature and pressure. The densities of CO_2 and ethane at each operating condition were calculated from density data obtained from the literature.[8,9]

3. Results and Discussion

3.1. Equilibrium Constant Determination. The C═O stretching bands of formic acid monomer and dimer appear at 1759 and 1731 cm^{-1}, respectively, as shown in Figure 3. Under the present experimental conditions, no oligomers (greater than dimer, linear chain) of formic acid were observed at the concentrations studied here. The C═O stretching band of the higher oligomers[1,10] were not observed in the FTIR spectra obtained. In addition, great care was taken to ensure the presence of essentially no water at 1644 cm^{-1} in the system,[11] and this was confirmed spectroscopically. The dimerization constant, K, was defined as

$$2\mathrm{FA} \overset{K}{\rightleftharpoons} (\mathrm{FA})_2 \quad K = [(\mathrm{FA})_2]/[\mathrm{FA}]^2 \qquad (1)$$

where $[(FA)_2]$ and [FA] are designated as a concentration of formic acid dimer and monomer, respectively. The total

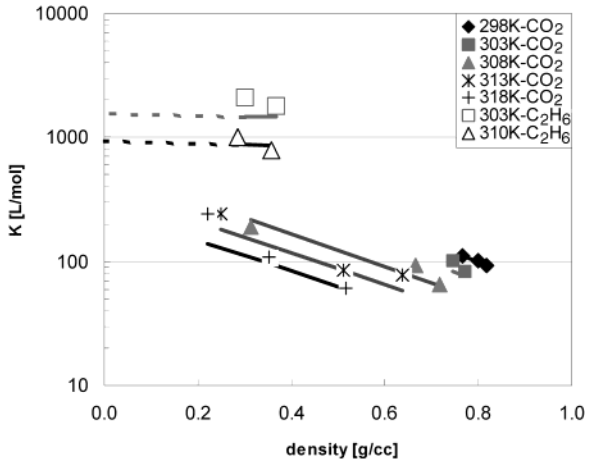

Figure 4. Variation of *K* with density along different isotherms in carbon dioxide and ethane solvents. The solid line indicates the MLFHB modeling results.

concentration of the formic acid, *C*, is

$$C = [\mathrm{FA}] + 2[(\mathrm{FA})_2] \tag{2}$$

To obtain the concentration of the dimer and monomer of formic acid, the method developed by Fujii and co-workers[4] for acetic acid was used directly. Here we assume that self-association of the formic acid results in only the dimer and no higher order oligomers. Given the dilute concentrations of formic acid employed here, it is also presumed that the Lambert−Beer law pertains for the carbonyl bands of both the acid monomer and dimer. The peak areas for the monomer and dimer, A_m and A_d, respectively, are given by

$$A_m = \epsilon_m * l * [\mathrm{FA}] \tag{3}$$

$$A_d = \epsilon_d * l * [(\mathrm{FA})_2] \tag{4}$$

where *l* is the cell path length and ϵ is the molar extinction coefficient of the band. Once the FTIR spectra were obtained at a given set of conditions, a commercial software package, PeakSolve (Galactic Industries Corp.), was used to curve-fit the collection of peaks to obtain the separate peak areas for the monomer (A_m) and dimer (A_d). The Voigt peak shape, a combination of Gaussian and Lorentzian peak shapes, was used for all peaks. The peak center, height, Gaussian width, and Lorentzian width for each peak were optimized to fit the FTIR spectrum.

The values of ϵ_m and ϵ_d are necessary for the calculation of *K*. Rearrangement of the eqs 2−4 yields

$$C*l/A_m = 1/\epsilon_m + (2/\epsilon_d)(A_d/A_m) \tag{5}$$

Molar extinction coefficients for monomer and dimer of formic acid at a given temperature and pressure were obtained from the intercept and slope of a plot of $C*l/A_m$ versus A_d/A_m. The dimerization constants obtained by eqs 1−5 are shown in Figure 4 and Table 2.

3.2. Formic Acid in CO_2. Figure 4 presents the dimerization constants, *K*, of formic acid as a function of solvent density in carbon dioxide. The *K* values shown in Figure 4 represent averaged values of duplicate runs at a given temperature and density over the formic acid concentrations in this study. The experiments were performed twice at each experimental condition, and experimental results performed produced similar *K* values with less than 10% variation. No systematic variation of *K* with concentration at a fixed temperature and density was apparent. The dimerization constants were determined at formic acid concentrations ranging from 1.0 to 8.4 mmol/L. The results in Figure 4 indicate that the dimer formation is more preferred in the low-density CO_2 and log *K* decreases nearly linearly with increasing density (pressure) along an isotherm. For example, *K* decreases from 240 L/mol at 0.222 g/cm^3 density to 61 L/mol at 0.518 g/cm^3 density along the 318 K isotherm. In addition, *K* decreases with an increase in temperature at a given density (e.g., *K* decreases from 86 to 61 L/mol by changing the temperature from 313 to 318 K at a density of approximately 0.5 g/cm^3). Similar phenomena are reported by Kazarian et al.[12] on the hydrogen-bonding equilibrium between perfluoro-*tert*-butyl alcohol (PFTB) and dimethyl ether (DME) in solution in SF_6 (T_c = 45.5 °C, P_c = 540 psi, ρ_c = 5.03 mol/L). They outlined the thermodynamics behind this density dependence. Their explanation can be summarized as stating that solvation energies become increasingly important as the density of the fluid increases. This linear dependence of log *K* on the fluid density observed in this study was also modeled here to obtain theoretical values of *K* in the sub- and supercritical solvents CO_2 and C_2H_6 as discussed in the following sections.

It should be pointed out that *K* values were originally calculated through an alternative method.[13] In this alternative method, the concentrations of monomer and dimer of formic acid were estimated simply using the maximum peak absorbance instead of peak areas. The formic acid dimerization *K* values obtained through this simple method were about 25% smaller than those obtained using the peak area method. This result is in agreement of with that of Meredith et al.[14]

TABLE 1: LFHB Scaling Parameters[a] for Pure Fluids[24]

fluid	T^* (K)	P^* (MPa)	ρ^* (kg/m^3)
methanol	496	315	786
ethanol	464	328	826
water	518	475	853
ethane	315	327	640
Carbon dioxide	305	574	1510

[a] T^* = characteristic temperature, P^* = characteristic pressure, and ρ^* = characteristic density.

TABLE 2: Formic Acid Dimerization Constants in CO_2 and C_2H_6 at Various Conditions

solvent	*T* (K)	*P* (bar)	ρ (g/cm^3)[a]	calcd *K* (L/mol)[b]	measd *K* (L/mol)
CO_2	298	75	0.766	110	111
	298	88	0.799	99	103
	298	100	0.817	95	94
	303	75	0.680	100	75
	303	88	0.745	83	100
	303	100	0.772	77	83
	308	75	0.313	215	191
	308	88	0.667	74	92
	308	100	0.716	64	65
	313	75	0.249	183	240
	313	88	0.510	85	86
	313	100	0.637	59	78
	318	75	0.222	140	240
	318	88	0.351	97	108
	318	100	0.518	60	61
C_2H_6	303	48	0.302	1466	2080
	303	88	0.367	1466	1808
	310	63	0.285	880	1002
	310	100	0.358	871	796

[a] Densities of CO_2 and C_2H_6 were estimated from refs 8 and 9, respectively. [b] Calculated dimerization constant, *K*, was obtained by using eq 6.

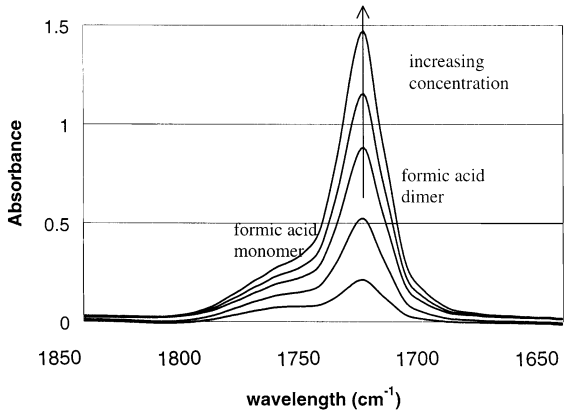

Figure 5. FTIR spectra of the C═O stretching band for formic acid in ethane at 303 K and 88 bar.

3.3. Formic Acid in Ethane. Upon a change of the solvent medium from CO_2 to C_2H_6, dramatic changes in the absorbances of the carbonyl stretching bands for the monomer and dimer of formic acid in C_2H_6 were obtained, as shown in Figure 5. This figure qualitatively presents that the absorbance of formic acid dimer in C_2H_6 is significantly higher than that in CO_2 at a given set of conditions (temperature and density). Such a large absorbance of formic acid dimer in C_2H_6 is the result of a dramatic increase in the dimerization constant at a given set of conditions compared to that in CO_2.

As in the CO_2 system, the dimerization constant at the higher density of C_2H_6 is lower than that in the lower density C_2H_6. The available surface area in the higher density medium is limited and hence hinders the formation of the dimer of formic acid. Once again, K decreases with an increase in temperature at a given density in C_2H_6 solvent as it did in CO_2. When the solvent was changed from CO_2 to ethane, the dimerization constant, K, was dramatically increased by 1 order of magnitude as shown in Figure 4. The formic acid monomer is much more stable in CO_2 than in ethane as a result of the stronger interactions between CO_2 and the formic acid monomer. Similar results were obtained for other hydrogen-bonding systems in CO_2 compared to in hydrocarbons.[6,7] These experimental results for the temperature and density dependence of K in the two different media were also modeled as discussed below.

3.4. Modeling. A number of hydrogen-bonding theories have been proposed in the literature.[15−22] In this study, we have used a modified lattice-fluid hydrogen-bonding (MLFHB) theory[20−22] because it reflects the effect of a dense solvent reasonably well. The general form of the MLFHB model can be somewhat simplified for the formic acid system because formic acid has a single donor site, and within the concentration range used in this study, formation of formic acid oligomers can be ignored. For dilute concentrations,[23] the dependence of the equilibrium constant, K, on the temperature, T, pressure, P, and reduced density, ρ_r, can be expressed as

$$RT \ln K = RT \ln v^* - E^\circ - PV^\circ + TS^\circ - \rho_r F' \qquad (6)$$

where R is the gas constant, v^* is the lattice-fluid close-packed segment volume, and E°, V°, and S° are the standard enthalpy, volume, and entropy change upon hydrogen bond formation, respectively. The close-packed segment volume is related to the lattice-fluid characteristic parameters P^* and T^* according to the relationship $v^* = RT^*/P^*$. Given the conditions applicable to our experiments, it is the final term in eq 6 that largely determines the dependence of ln K on solvent density. A detailed development of these equations from LFHB is shown elsewhere.[13,22]

TABLE 3: LFHB Parameters[a] for Formic Acid Association

parameter	estimated value
E°	−58.8 kJ/mol
S°	−151 J/(mol/K)
V°	−10.0 cm^3/mol

[a] E° is enthalpy change upon hydrogen bond formation. S° is entropy change upon hydrogen bond formation. V° is volume change upon hydrogen bond formation.

Three lattice-fluid scaling parameters (P^*, T^*, and ρ^*) are required only for the solvents of CO_2 and C_2H_6 since the concentration of formic acid is dilute. Four hydrogen-bonding parameters (E°, S°, V°, and F') are needed for formic acid dimerization. The three lattice-fluid parameters (listed in Table 1) required for CO_2 and C_2H_6 were obtained from the literature.[24] For the formic acid hydrogen bond, the E° and S° parameters (Table 3) were also obtained from the literature.[25] The value of parameter V° was fixed at a typical value of −10 cm^3/mol [12] to reduce the number of parameters regressed from the experimental data. The value of the parameter F' was obtained from the plot of log K versus density at the temperatures ranging from 298 to 313 K. This approach is convenient since gas-phase values are widely available.

For each isotherm, a significant increase in K is observed as density decreases, as was also observed for the PFTB/DME/SF_6 system.[12] The dependence of log K on ρ is close to linear and can be modeled convincingly by the MLFHB model (solid line in Figure 4). The dashed line in Figure 4 represents an extrapolation to the gas-phase value. In both the modeling and experimental results, as solvent density is increased, the K values decrease along a given isotherm. This is possibly due to an energetic effect between formic acid and solvent molecule and the loss of interaction surface area upon hydrogen bonding. In other words, the dimer formation is more preferred in the low-density solvent, while the high-density solvent interacts strongly with the monomer thereby reducing dimer formation. According to these results, the dimer formation is more preferred in the low-density solvent (CO_2 and C_2H_6) than in high density. Also, as temperature is increased at a given solvent density, the equilibrium constant decreases in both the modeling and experimental results. This can be attributed to the decrease in hydrogen bonding between monomers at elevated temperatures.[21]

Gas-phase values of the dimerization equilibrium constant of formic acid are available in the literature at various temperatures.[25] As an example, the gas phase K value at 313 K is 84.2 (unitless). The unitless K can be related to K in L/mol through the following relation: K (unitless) = K (L/mol)/v^*. Figure 6 shows the results of the MLFHB model predictions at 313 K when the model is anchored at the gas phase K value of 84.2 (unitless) or 828.7 L/mol using the value of v^* as the adjustable parameter. The resulting value of v^* is 9.84 cm^3/mol, which is consistent with the v^* value of a similar molecular weight hydrocarbon, propane.[26] In MLFHB, H-bonding is separated from physical interactions. v^* represents hard core volume considering only physical interactions of formic acid, which is similar that of propane. When anchored at the gas phase value, the equilibrium constants are greatly over predicted at the higher densities but match more closely at the low density of 0.2 g/cm^3. This result further suggests that the higher density carbon dioxide hinders formic acid dimer formation due to the interactions between solute and solvent.

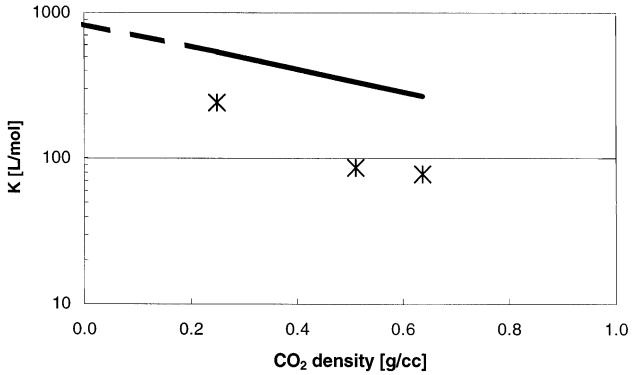

Figure 6. Variation of *K* with carbon dioxide density at 313 K. The solid line indicates the MLFHB modeling results anchored at the gas-phase *K* value of 828.7 L/mol.

TABLE 4: Comparison of Estimated Free Energy Change upon Hydrogen Bonding in Different Systems

system	F' (kJ/mol)
formic acid/CO_2	11.5
formic acid/C_2H_6	0.5
PFTB/DME/SF_6[a]	3.0

[a] Reference 12.

The effect of changing the solvent is also evident as shown in Figure 4. The dimerization constant in ethane is 1 order of magnitude higher than in CO_2 at the density of 0.3 g/cm^3. This result indicates that the formic acid monomer is much more stable in CO_2 than in ethane as a result of the interactions between CO_2 and the formic acid monomer. Kazarian et al.[27] and Reilly et al.[28] reported the effects of interactions between CO_2 and various carbonyl-containing compounds that could contribute to the phenomena observed here. The carbon in CO_2 may serve as a Lewis acid to accept the electrons from either the oxygen of carbonyl group or the oxygen in the hydroxyl group of formic acid. The experimental values of *K* in ethane are consistent with the literature gas phase *K* values. As an example, the range of *K* values in ethane at 303 K is from 1808 to 2080 L/mol where the gas phase *K* value at 303 K is 1747 L/mol (177.5 unitless).[25]

The modeling results obtained were compared to that provided by Kazarian et al.[12] for the system of PFTB/DME/SF_6. The free energy change upon hydrogen bonding, F', is a positive value in all three systems, as shown in Table 4. It follows that increasing density will cause a reduction in *K* and, hence, shift toward free formic acid at equilibrium. The free energy change in the system of formic acid in ethane is only 0.5 kJ/mol, and that in the system of PFTM/DME/SF_6 is just 3 kJ/mol. This suggests that there may be a significant interaction between formic acid (solute) and CO_2 (solvent) on the basis of the free energy change of more than 10 kJ/mol.

4. Conclusions

Fourier transform infrared (FTIR) spectroscopy was used to determine the equilibrium constants of dimerization between formic acid dimer and monomer in CO_2 and ethane. In general, the results show that an increase in solvent (CO_2 and C_2H_6) density causes an increase in the concentration of the formic acid monomer, which results in a decrease in *K*. The interaction of CO_2 (solvent) with formic acid (solute) has a marked effect on the dimer formation compared to that in ethane, which causes the dimerization constant in C_2H_6 to be much larger than that in CO_2. Additionally, using the modified lattice-fluid hydrogen bonding (MLFHB) model, this behavior has been successfully modeled and log *K* decreases almost linearly with increasing fluid (CO_2 and C_2H_6) density at constant temperature.

Acknowledgment. C.B.R. thanks the Auburn University Biogrants Program and The Department of Energy, Basic Energy Sciences (Grant DE-FG02-01ER15255), for financial assistance. We are also grateful to Dr. Vince Cammarata (Chemistry Department), Mr. J. Paul Pathasema (Chemical Engineering Department), and Mr. Ronald S. Ramsey (Space Power Center) for their help.

References and Notes

(1) Ramon, J. M. H.; Rios, M. A. *Chem. Phys.* **1999**, *250*, 155.
(2) Allen, G.; Watkinson, J. G.; Webb, K. H. *Spectrosc. Acta* **1966**, *22*, 807.
(3) Bulmer, J. T.; Shurvell, H. F. *J. Phys. Chem.* **1973**, *77*(2), 256.
(4) Fujii, Y.; Yamada, H.; Mizuta, M. *J. Phys. Chem.* **1988**, *92*, 6768.
(5) Tsugane, H.; Yagi, Y.; Inomata, H.; Saito, S. *J. Chem. Eng. Jpn.* **1992**, *25*(3), 351.
(6) Yamamoto, M.; Iwai, Y.; Nakajima, T.; Arai, Y. *J. Phys. Chem. A* **1999**, *103*, 3525.
(7) Fulton, J. L.; Yee, G. G.; Smith, R. D. *J. Am. Chem. Soc.* **1991**, *113*, 8327.
(8) Angus, S.; Armstrong, B.; Reuk, K. *International Thermodynamics Tables of the Fluid State of Carbon Dioxide*; Pergamon Press: Elmsford, NY, 1976.
(9) Sychev, V. V.; Selover, T. B.; Slark, G. E. *Thermodynamic Properties of Ethane*; Hemisphere Publishing Corp.: New York, 1987.
(10) Stein M.; Sauer J. *Chem. Phys. Lett.* **1997**, *267*, 111.
(11) Schultz, C. P.; Eysel, H. H.; Mantsch, H. H.; Jackson, M. *J. Phys. Chem.* **1996**, *100*, 6845.
(12) Kazarian, S. G.; Gupta, R. B.; Clarke, M. J.; Johnston, K. P.; Poliakoff, M. *J. Am. Chem. Soc.* **1993**, *115*, 11099.
(13) Park, Y. Ph.D. Thesis, Auburn University, 2000.
(14) Meredith, J. C.; Johnston, K. P.; Seminario, J. M.; Kazarian, S. G.; Eckert, C. A. *J. Phys. Chem.* **1996**, *100*, 10837.
(15) Heidemann, R. A.; Prausnitz, J. M. *Proc. Natl. Acad. Sci. U.S.A.* **1976**, *73*, 1773.
(16) Economou, I. G.; Donahue, M. D. *AIChE J.* **1991**, *37*, 1875.
(17) Huang, S. H.; Radosz, M. *Ind. Eng. Chem. Res.* **1990**, *29*, 2284.
(18) Huang, S. H.; Radosz, M. *Ind. Eng. Chem. Res.* **1993**, *32*, 762.
(19) Huyskens, P. L. *J. Mol. Struct.* **1992**, *274*, 223.
(20) Panayiotou, C.; Sanchez, I. C. *J. Phys. Chem.* **1991**, *95*, 10090.
(21) Gupta, R. B.; Brinkley, R. L. *AIChE J.* **1998**, *44*(1), 207.
(22) Gupta, R. B.; Panayiotou, C. G.; Sanchez, I. C.; Johnston, K. P. *AIChE J.* **1992**, *38*(8), 1243.
(23) Gupta, R. B.; Combes, J. R.; Johnston, K. P. *J. Phys. Chem.* **1993**, *97*, 707.
(24) Xiong, Y.; Kiran, E. *Polymer.* **1994**, *35*(20), 4408.
(25) Coolidge, A. *J. Am. Chem. Soc.* **1928**, *50*, 2166.
(26) Sanchez, I. C.; Lacombe, R. H. *Macromolecules* **1978**, *11*, 1145.
(27) Kazarian, S. G.; Vincent, M. F.; Bright, F. V.; Liotta, C. L.; Eckert, C. A. *J. Am. Chem. Soc.* **1996**, *118*, 1729.
(28) Reilly, J. T.; Bokis, C. P.; Donohue, M. D. *Int. J. Thermophys.* **1995**, *16*, 599.